International Journal of Applied Pharmaceutics

ISSN- 0975-7058 Vol 16, Issue 6, 2024

Original Article

DEVELOPMENT OF GABAPENTIN-LOADED SOLID LIPID NANOPARTICLE FOR ALLEVIATING SEIZURE ACTIVITY IN PICROTOXIN AND BICUCULLINE-INDUCED RATS

POOJA AGARWAL*, VASUDHA BAKSHI

*School of Pharmacy, Anurag University, Venkatapur, Ghatkesar, Medchal-Malkajgiri, Hyderabad, Telangana, India
*Corresponding author: Pooja Agarwal; *Email: pharmacy.pooja.agarwal@gmail.com

Received: 15 May 2024, Revised and Accepted: 12 Aug 2024

ABSTRACT

Objective: The current research aimed to prepare gabapentin-loaded Solid Lipid Nanoparticles (SLN) for alleviating seizure activity in picrotoxin and bicuculline-induced Wistar rats.

Methods: Gabapentin-loaded SLNs were formulated using a Box-Behnken experimental design with three-level three-factor consisting of 17 experimental runs by micro-emulsification. Three independent parameters were considered in this study, namely sodium glyceryl tripalmitate (A), RPM (B), and Poloxamer-188 (C). Particle size, drug release, and Encapsulation Efficiency (EE) as dependent variables. The formulation was evaluated for drug release, EE, Attenuated Total Reflection (ATR), Differential Scanning Calorimetry (DSC), X-ray diffraction (XRD), surface morphology, particle size, zeta potential, *in vivo* anti-convulsion study.

Results: The data collected during the experiment includes the measurements of EE (Encapsulation Efficiency), drug release at the 12th h, and particle size. It was reported that formulations containing a high concentration of Glyceryl tripalmitate (50%) had a high Encapsulation Efficiency (EE). The *in vitro* release results indicate that F17 demonstrated a maximum drug concentration of 99.99% within a 12 h. The optimization process was conducted using mathematical and graphical methods. From ATR spectra, it was found that there are no such major interactions between gabapentin and excipients. A significant endothermal peak was seen in the DSC investigation at 208.81 °C. X-ray diffraction revealed that gabapentin was present in the crystalline form. Drug crystals and SLN were seen to be dispersed and scattered from Scanning Electron Microscope (SEM). The optimized formulation's particle size was found to be 203.4 nm, the Polydispersity Index (PI) of 0.426, and the zeta value of 16.5 mV; indicating stability. Following a lethal and chronic dosage of picrotoxin, the gabapentin-SLN exhibited a higher anticonvulsant efficacy, according to *in vivo* research on rats ($p<0.05$).

Conclusion: Compared to the Bicuculline model, the optimized SLN demonstrated superior outcomes regarding seizure initiation in the Picrotoxin-induced convulsion.

Keywords: Gabapentin, Box-behnken design, Solid lipid nanoparticle, Glyceryl tripalmitate, Poloxamer-188, *In vitro* release, *In vivo* anti-convulsion study

DOI: https://dx.doi.org/10.22159/ijap.2024v16i6.51157 Journal homepage: https://innovareacademics.in/journals/index.php/ijap

INTRODUCTION

Epilepsy manifests as a condition where an individual experiences recurrent, unprovoked seizures. A seizure can be defined as a transient event marked by abnormal, excessive, or synchronized neuronal activity [1, 2]. Roughly 50 million individuals worldwide are affected by epilepsy, making it one of the most widespread neurological disorders on a global scale. Nearly 80% of those grappling with epilepsy resides in low-and middle-income countries [3]. Seizures are paroxysmal expressions of the cerebral cortex. An abrupt imbalance between the excitatory and inhibitory forces within the network of cortical neurons causes a seizure [4]. None of the Anti-Epileptic Medicines (AEDs) has demonstrated maximum effectiveness in treating epilepsy, and each AED has its unique combination of negative side effects.

AEDs are chosen based on adverse effects, ease of administration, cost-effectiveness, and medical professionals' familiarity with the medicine [5]. The Blood-Brain Barrier (BBB) and drug interactions with AEDs are often the two problems that the anti-epileptic medication must deal with. The main difficulties in treating epilepsy stem from a drug's limited capacity to cross the blood-brain barrier and its low bioavailability. Only tiny molecules, including lipid-soluble ones and those with a molecular weight of 400–600 Da, diffuse through the BBB. Simultaneously, small molecules with a molecular weight of 400–600 Da or those that are soluble in water are poorly transported via the BBB [6]. Unionized compounds with log P values around 2, molecular weights around 400 Da, and no more than 8–10 hydrogen bonds can traverse the BBB optimally [7]. A selective metabolism-driven barrier exists in addition to the physical barrier, reflecting the presence and operation of several receptors, ion channels, and protein transporters [8]. The drawbacks of AEDs are that the antiepileptic medications that are now on the market are insufficient, and their side effects make inpatient administration difficult. Antiepileptic drugs only have a symptomatic effect on seizure symptoms and do not affect epileptogenesis. Antiepileptic drug use is restricted due to its adverse effects, withdrawal symptoms, harmful interactions with other medications, and high cost, especially in developing countries [9].

Various methods have been explored to improve brain drug delivery, including invasive procedures like injecting drugs directly into the brain's ventricles or using implanted devices, each with its effectiveness and risks [10, 11]. Hence, there is a requirement for innovative drug delivery strategies capable of crossing the BBB without causing harm to brain cells, and this is where nanomedicine comes into play [12]. The various physicochemical features of treatments pose a challenge in the development of nanocarriers for medication delivery. Solid Lipid Nanoparticles (SLNs) are physiological lipid-based delivery systems that possess unique properties such as small size, large surface area, high drug loading, and phase interaction at the interfaces. These properties provide physical stability, protection of labile drugs from degradation, ease of preparation, and lower toxicity; consequently, they have the potential to enhance the efficacy of pharmaceuticals, nutraceuticals, and other materials [13]. In place of the current conventional carriers, such as liposomes and polymeric NPs, SLNs have been developed as an alternate delivery method. Solid-lipid emulsions are a new class of lipid emulsions in which a solid lipid has replaced the liquid lipid [14]. Targeted drug delivery using SLNs has advanced significantly recently against a range of diseases, including cancer and neurological illnesses like epilepsy [15]. The primary goal of the current study is to use the Box-Behnken design of experiments to create solid lipid nanoparticles of gabapentin.

MATERIALS AND METHODS

Materials

Gabapentin was received as a gift sample from Aurobindo Pharma, Hyderabad. Glyceryl tripalmitate, Sunflower lecithin, and Poloxamer-188 were obtained from Sigma Aldrich (St. Louis, MO, USA). All the reagents used were of analytical grade.

Methods

Preparation of solid lipid nanoparticle

The present study involves the preparation of SLN containing gabapentin seventeen formulations through microemulsification. The initial amount of gabapentin, along with glyceryl tripalmitate (a lipid), was dissolved in an organic solvent (ethanol) at a temperature of 45 °C. In addition, sunflower lecithin was introduced as a co-emulsifier to the solution mentioned above. Another beaker was used to prepare an aqueous poloxamer solution 188, with a temperature of 45 °C, similar to the previous experiment. The lipophilic drug phase was introduced into the aqueous phase while maintaining constant stirring at a specified rotation per minute (as indicated in the accompanying table), resulting in the formation of a primary oil-in-water emulsion [16, 17]. In addition, the coarse emulsion underwent a 10-minute ultrasonication process utilizing a probe sonicator (UAI-PS20khz-900W, Ultra Autosonic, India) at an amplitude of 45% for the same duration. To produce SLN, the dispersion was freeze-dried for 24 h at-80 °C using a lyophilizer (BK FD10, Biobase, China). Subsequently, the SLN was stored at a temperature of 4 °C for subsequent assessment and processing.

Box-behnken design (BBD)

To evaluate the effect of specific independent variables on the replies, the current study used a Box-Behnken experimental design with three levels and three factors. This study took into account three independent parameters: sodium glyceryl tripalmitate (A), RPM (B), and Poloxamer-188 (C). Particle size, drug release at the 12 h mark, and EE (encapsulation efficiency) measures are among the information gathered during the experiment. For mathematical fitting and analysis, the polynomial equation was used [18, 19]. Using a confidence interval value of alpha 0.05, the best formula was found by applying a numerical method along with a graphical optimization strategy. There were 17 experimental runs in the three-level, three-factor Box-Behnken experimental design.

Characterization of SLNs

A properly measured quantity of SLN, equivalent to 50 mg of the drug, was placed in a 100 ml volumetric flask. The minimum amount of ethanol was then added and the mixture was thoroughly stirred. The dispersion was subjected to sonication using an Ultrasonicator (model CPX3800-E, Branson) for approximately 10 min. A phosphate buffer solution with a pH of 6.8 was introduced into the resulting combination, and the volume was subsequently modified to achieve the intended level [20]. The dispersion underwent an additional 10 min bath sonication process until it achieved a state of transparency. The resultant mixture underwent filtration using a Whatman membrane filter with a pore size of 0.45 m. To determine the amount of drug present, the filtrate underwent analysis using a UV-visible spectrophotometer (Shimadzu UV-1800, Japan) at a wavelength of 335 nm. The percent Entrapment Efficiency (EE) and Drug Loading (DL) were determined using the provided formulas.

Drug loading

$$\text{DL } (\%) = \frac{\text{Drug content in SLNs}}{\text{Total weight of SLNs}} \text{ x } 100 \text{ ..... (Eq. 1)}$$

$$\text{Entrapment efficiency: EE } (\%) = \frac{\text{Mass of drug in SLNs}}{\text{Initial mass of drug used in SLNs}} \text{ x } 100 \text{ .... (Eq. 2)}$$

In vitro drug release

Gabapentin was released from the SLNs *in vitro* via the diffusion procedure with a Franz-diffusion cell. Before use, the cellophane dialysis membrane was cut into equal pieces of 6 cm by 2.5 cm and soaked in distilled water for 12 h. The gabapentin drug release tests are conducted in 10 milliliters of pH 6.8 saline buffer, which is maintained at 37±0.5° using a magnetic stirrer and continuous heating equipment (IKA Auto Temp Regulator, Germany). Two milliliters of the SLN suspension sample were added to the receptor compartment. At regular intervals, 1 ml aliquot samples were removed and replaced with the same volume of brand-new buffer. If required, fresh medium was added to the aliquots [21]. Using phosphate buffer (pH 6.8) as the blank and a UV spectrophotometer set to 335 nm, the amount of medication that had diffused through the membrane was quantified.

ATR study of drug and excipients

When combined with infrared spectroscopy, Attenuated Total Reflection (ATR) sampling allows materials to be analyzed *in-situ*, either solid or liquid, without the need for additional preparation. Online monitoring of polymer composition is a particularly valuable application of ATR spectroscopy [22]. IR can identify the components of a chemical process because of its capacity to fingerprint chemical components. The German company ATR Bruker Opus 7.0 was used to carry out the investigation.

Differential scanning calorimetry (DSC) study

A thermal analysis tool called DSC measures a sample's physical characteristics and temperature over time [23]. Stated differently, the apparatus is a thermal analysis tool that measures the temperature and heat flux related to material transitions about temperature and time. DSC-60, Shimadzu, USA, was used to perform DSC.

X-ray diffraction (XRD) study

The structure of crystalline materials can be examined non-destructively using X-Ray Diffraction, or XRD for short [24]. By examining the crystal structure of a material, XRD analysis may determine which crystalline phases are present and, therefore, provide details about the chemical composition of the material. Thermo Scientific, India's ARL EQUINOX 100 was used to conduct the XRD research.

Surface morphology, particle size, and zeta potential of optimized formulation

Using a scanning electron microscope, the morphology of the synthesized and optimized gabapentin-loaded Solid Lipid Nanoparticles (SLN) was investigated [25]. Using double-sided sticky tape, the specimen was attached to the slab surface, and photomicrographs were taken with the Scanning Electron Microscope (SEM) (S3700N-Hitachi, Japan) at different magnifications. Similar to this, the scattering light intensity was used to determine the particle size and polydispersity index value of the SLN (Malvern Zetasizer, ATA Scientific, USA).

In vivo anti-convulsion study by picrotoxin and bicuculline induced convulsion

The research was conducted in conformity with the guidelines set forth by the Committee for the Purpose of Control and Supervision of Experiments on Animals (CPCSEA). Before conducting the *in vivo* investigation, the research project obtained approval from the Institutional Animal Ethical Committee, with the assigned approval number CPCSEA/IAEC/JLS/19/02/23/157.

The animal study was conducted at Jeeva Life Sciences, Hyderabad, Telangana, India. Before conducting the study, Wistar rats weighing between 200-250 g were selected and subsequently separated into six distinct groups [26]. The subjects were given a time of 10 days to acclimate further, during which they were closely monitored to detect any indications of stress. In Group I, the rats were provided with a standard diet for their health. In the Group II experiment, rats were subjected to the administration of "picrotoxin/bicuculline" following the specified quantities outlined in tables 5 and 6, to induce seizures. In Group III, the standard medicine diazepam was supplied at a dosage of 0.5 mg/kg, in combination with picrotoxin/bicuculline. On the other hand, Groups IV, V, and VI received the optimized formulation orally, using an 18-gauge ball-tipped gavage needle. The dosage strength exhibited a progressive increase, ranging from 5.0 mg/kg to 50.0 mg/kg, in the optimized formulation.

The mean start of seizure, characterized by the emergence of unilateral forelimb clonus, as well as the length of seizure and time to death, were documented. Both picrotoxin and bicuculline are known to elicit seizures by acting as antagonists of the neurotransmitter GABA. Nevertheless, the function of the chloride ion channel of the GABA complex is altered by picrotoxin.

RESULTS AND DISCUSSION

The development of sustained-release drugs has advanced significantly due to recent breakthroughs in nanotechnology. The primary goal of the therapy is to efficiently focus drugs on the tissue, resulting in reduced side effects and improved effectiveness. It is vital to cross the blood-brain barrier, particularly in cases of central nervous system problems. Because of this, various dosage forms and application methods are being studied; one non-invasive method is nasal delivery of drug molecules. Pharmaceutical product quality problems are frequently linked to the design phase. A badly designed product is harmful and/or ineffective no matter how much testing is done. Instead of depending only on analysis and testing, including quality in the product design process is crucial. Historically, the development and optimization of pharmaceutical products have been accomplished by factor analysis. Here, one element is changed while the rest remain the same. Nevertheless, this approach takes a lot of time and prevents assessing potential factor interactions. This may result in formulation development and optimization being carried out insufficiently. The DoE technique can yield superior results with fewer experiments, circumventing these restrictions. DoE can assist in identifying interactions and streamlining the formulation development process by analyzing several elements at once.

The microemulsification and ultrasonication process was used to formulate seventeen different gabapentin-SLN formulations (F1–F17). Table 1 contains a list of the ingredients in the created formulations. The prepared gabapentin-SLN formulations were tested for EE%, particle size analysis, and *in vitro* release to choose the optimal formulation.

Table 1: Formulation details of gabapentin solid lipid nanoparticles

Formulations	Factor 1	Factor 2	Factor 3
	A: Glyceryl tripalmitate	B: RPM	C: Poloxamer-188
	mg	rpm	%
F1	115	2000	0.1
F2	200	3500	2
F3	200	5000	1.05
F4	115	2000	2
F5	115	3500	1.05
F6	200	2000	1.05
F7	115	3500	1.05
F8	115	3500	1.05
F9	200	3500	0.1
F10	30	5000	1.05
F11	115	5000	2
F12	115	3500	1.05
F13	115	5000	0.1
F14	30	2000	1.05
F15	30	3500	0.1
F16	115	3500	1.05
F17	30	3500	2

Table 2: The entrapment efficiency %, drug release at 12 h, particle size, and drug-loaded of 17 gabapentin solid lipid nanoparticle formulations; (n=3)

Formulations	Response 1	Response 2	Response 3	
	EE	Drug release at 12h	Particle size	Drug loaded
	%	%	Nm	%
F1	69.36±1.78	70.96±0.57	177.5±0.72	77.53±1.22
F2	72.93±0.42	64.85±0.29	182.6±0.59	83.13±0.66
F3	74.09±0.57	64.94±0.86	179.2±0.59	84.74±0.21
F4	66.15±0.55	84.36±0.71	172.1±0.31	77.22±0.84
F5	63.68±0.87	77.91±0.66	174.6±0.44	74.85±0.19
F6	83.32±0.73	67.52±0.41	191.3±0.60	91.26±0.16
F7	62.07±1.12	75.63±0.29	169.8±0.22	73.75±0.70
F8	64.26±0.50	74.85±0.23	168.3±0.24	75.25±0.60
F9	79.34±1.25	57.37±0.59	182.6±0.41	89.39±0.47
F10	48.96±0.34	98.93±0.63	151.8±0.08	59.58±0.41
F11	57.17±0.57	90.77±0.18	164.9±0.13	68.12±0.30
F12	64.08±0.94	74.54±0.22	168.2±0.35	74.47±0.41
F13	63.27±0.52	80.08±1.02	166.7±0.28	73.48±0.47
F14	54.84±0.61	91.59±0.27	160.3±0.09	65.17±0.86
F15	50.74±0.30	93.17±0.31	158.4±0.33	60.05±0.57
F16	65.22±0.84	72.34±0.33	169.6±0.57	75.24±0.29
F17	49.59±0.51	99.99±1.38	152.8±0.30	60.16±0.90

n= number of determinations; mean±Standard Deviation

Characterization of SLNs

It was reported that formulations containing a high concentration of glyceryl tripalmitate (50%) had a high Encapsulation Efficiency (EE). The formulation denoted as "F6" exhibits a maximum drug loading of 91.26 %, while formulations "F9" and "F3" have 89.39 % and 84.74 %, respectively. The percentage of poloxamer-188 in the formulations had a significant impact on the encapsulation

efficiency. Nevertheless, the inclusion of a substantial quantity of glyceryl tripalmitate in the Solid Lipid Nanoparticle (SLN) formulation resulted in the creation of a hydrophobic barrier that enveloped the drug molecule [27]. In conclusion, it can be inferred that the use of a judicious blend of glyceryl tripalmitate and poloxamer-188, in relatively smaller proportions, has the potential to yield SLNs with a commendable encapsulation efficiency. In contrast, the rotational speed of 2000 RPM resulted in the production of Solid Lipid Nanoparticles (SLN) with enhanced encapsulation efficiency, as seen by the "F6" formulation exhibiting an EE of 83.32%.

It can be difficult to load a hydrophilic drug into a lipophilic system, but maintaining high entrapment efficiency in drug delivery systems is crucial. Still, SLNs can capture both lipophilic and hydrophilic medications. In this work, the hydrophilic drug gabapentin was successfully loaded into SLNs.

In vitro drug release

Drug molecules must be released from SLNs to have therapeutic effects. Drug delivery systems must maintain a therapeutic concentration for efficient treatment; however, occasionally, the drug molecules adhere to the surface of the SLNs and are rapidly released into the surrounding medium. This phenomenon is referred to as a burst release.

In all of the formulations, it was observed that a maximum of 14% of the drug was released during the first 30 min. The results of the dissolving research indicate that F9 exhibited a minimum drug release of 57.37% within 12 h. In contrast, F17 demonstrated a maximum drug concentration of 99.99% within a 12 h time. An increased quantity of glyceryl tripalmitate resulted in a delayed release of the drug, while a higher quantity of poloxamer-188 accelerated the release of the drug. The amount of gabapentin released from SLNs can vary depending on the lipid matrix's composition and the proportion of surfactants utilized.

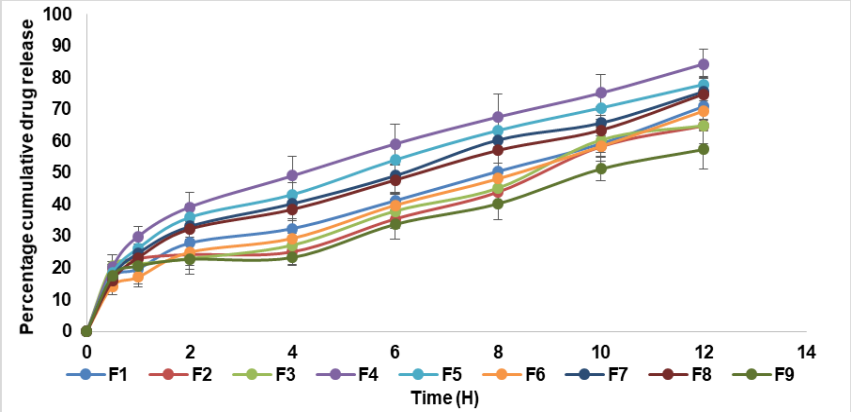

Fig. 1: % Release of gabapentin SLN (F1-F9) (n=3); n= number of determinations

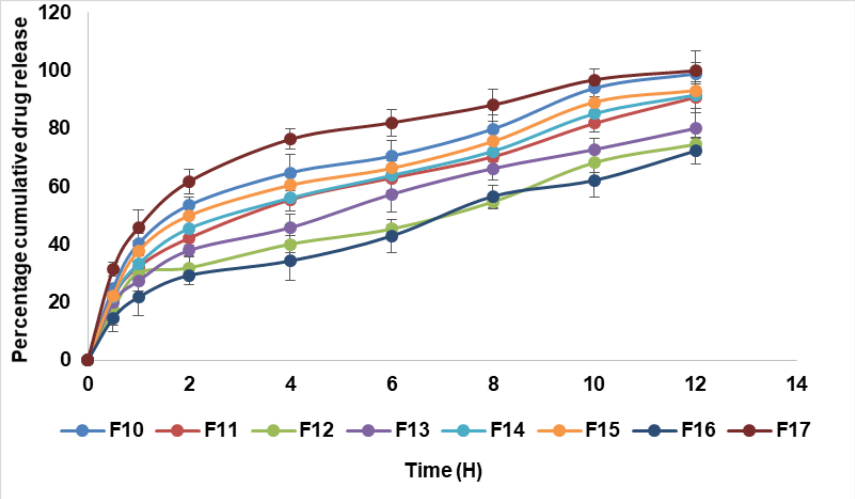

Fig. 2: % Release of gabapentin SLN (F10-F17) (n=3); n= number of determinations

It was noted that the formulations F2, F3, F6, and F9 had reduced drug release throughout 12 h due to their increased content (200 mg) of glyceryl tripalmitate. Based on the available literature, it has been shown that the hydrophobic nature of glyceryl tripalmitate can lead to the formation of a protective barrier around drug particles, hence impeding the rate of drug release [28]. A comparable release pattern can be noticed from the Revolutions Per Minute (RPM). A higher RPM results in a faster contribution compared to a lower RPM. The data reveals that F14 accounted for 91.59% of the drug, while F10 demonstrated a somewhat larger proportion of 98.93% of the medication. The elevated data may be attributed to a faster rotational speed during data processing.

Formulations suggested by box-behnken design (BBD)

$$\text{Response 1 [EE]} = 63.862 + 13.19A - 3.77B - 2.10C - 0.83AB - 1.31AC - 0.72BC - 0.30A^2 + 1.13B^2 - 1.01C^2 \quad \ldots\ldots\ldots\ldots\ldots\ldots (1)$$

In Response 1: Term A, Term B, Term C, AC, and B^2 are significant.

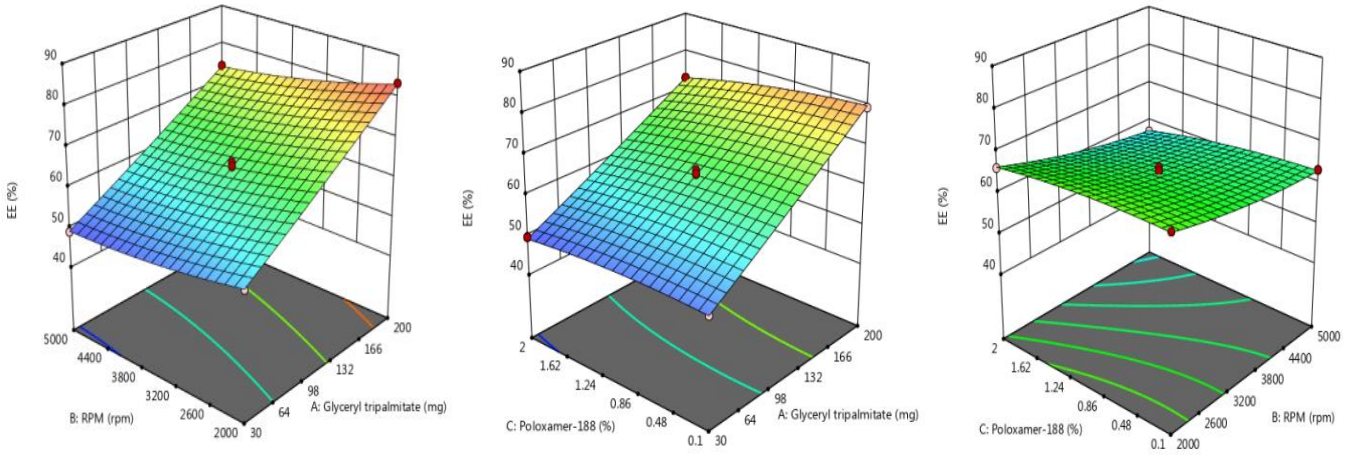

Fig. 3: 3D simulation curve of response 1(EE); Glyceryl tripalmitate Vs RPM, Glyceryl tripalmitate Vs poloxamer-188, Poloxamer-188 Vs RPM

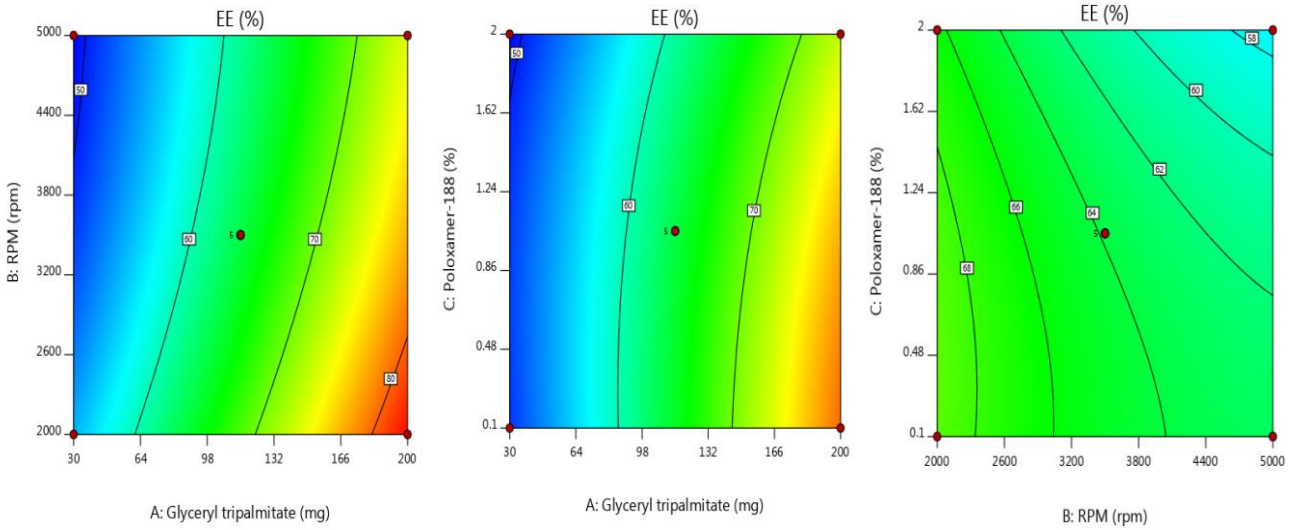

Fig. 4: 2D Contour plot of response 1(EE); Glyceryl tripalmitate Vs RPM, Glyceryl tripalmitate Vs Poloxamer-188, Poloxamer-188 Vs RPM

Response 2 [Drug released at 12th Hour] = 75.05-16.12A+2.53B+4.79C-2.48AB+0.16AC-0.67BC+1.49A^2+0.03B^2+2.29C^2…. (2)

In Response 2: Term A, Term B, Term C, and Quadratic term B^2 are significant.

Response 3 [Particle size] = 170.1+14.05A-4.82B-1.6C-0.9AB+1.4AC+0.9BC-0.32A^2+0.87B^2-0.67C^2…….. (3)

In Response 3: Term A, and Term B are significant

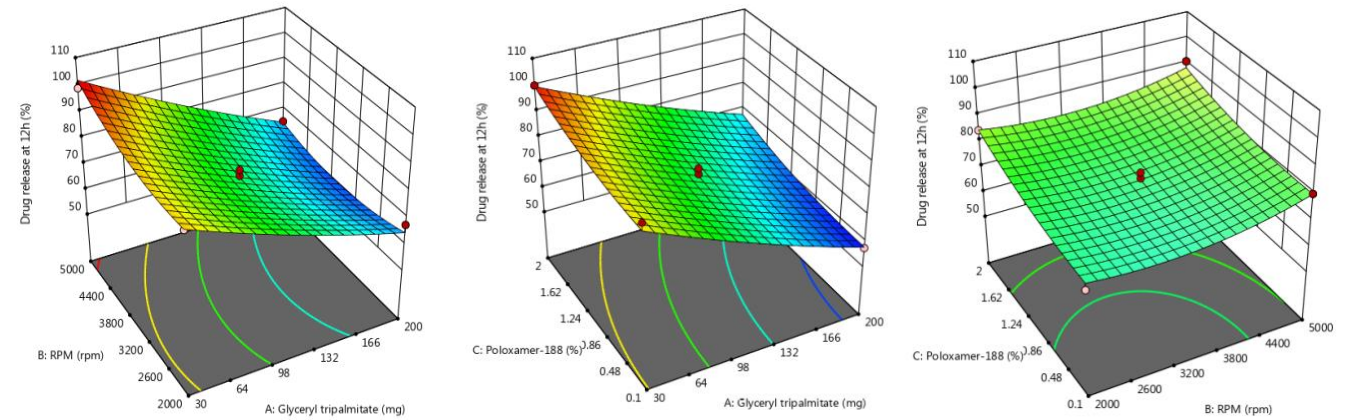

Fig. 5: 3D simulation curve of response 2(Drug released at 12th H); Glyceryl tripalmitate Vs RPM, Glyceryl tripalmitate Vs poloxamer-188, Poloxamer-188 Vs RPM

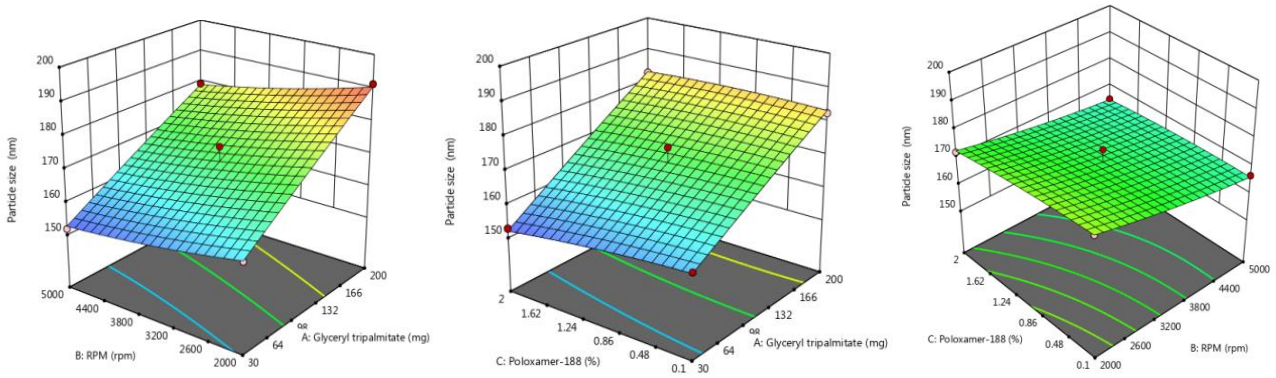

Fig. 6: 3D simulation curve of Response 3(Particle size); Glyceryl tripalmitate Vs RPM, Glyceryl tripalmitate Vs Poloxamer-188, Poloxamer-188 Vs RPM

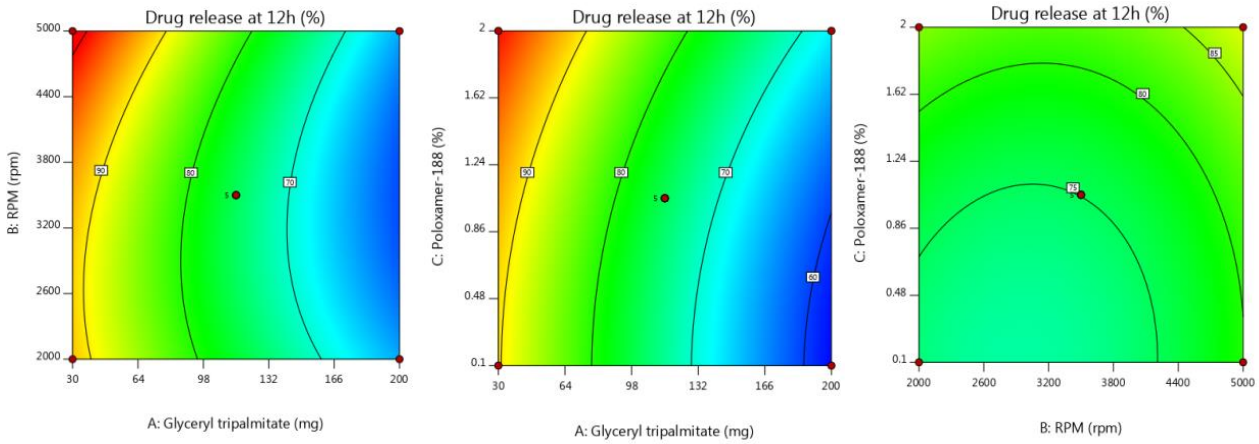

Fig. 7: 2D Contour plot of response 2(Drug released at 12th Hour); Glyceryl tripalmitate Vs RPM, Glyceryl tripalmitate Vs Poloxamer-188, Poloxamer-188 Vs RPM

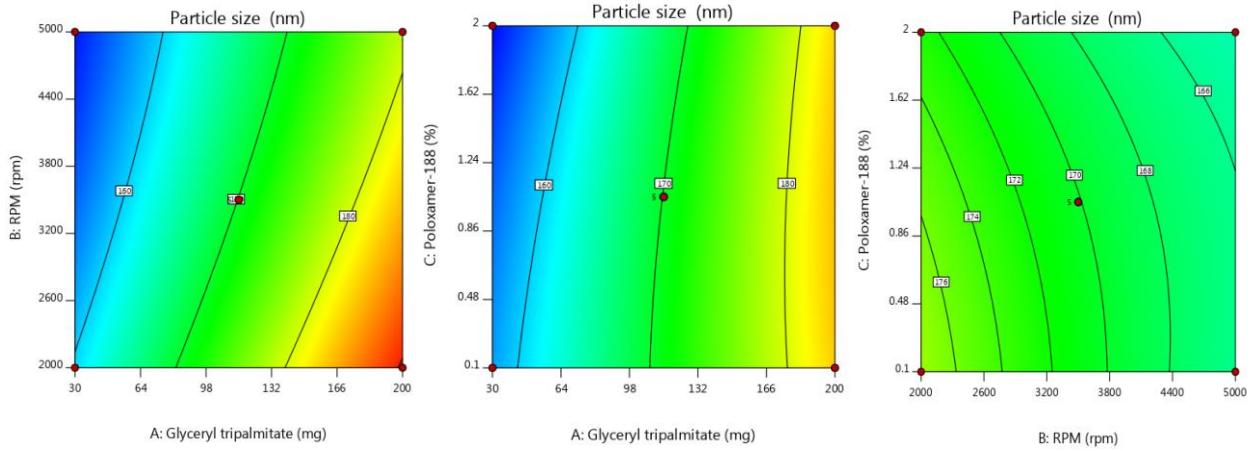

Fig. 8: 2D Contour plot of Response 3(Particle size); Glyceryl tripalmitate Vs RPM, Glyceryl tripalmitate Vs Poloxamer-188, Poloxamer-188 Vs RPM

Polynomial equation showed that terms such as A, B, and C are significant; similarly, the quadratic term, B2 is significant. However, it was found that only the interaction term AC is significant. Following the generation of the model polynomial equations, the process was optimized by considering the relationship between the dependent and independent variables. The application of canonical analysis determined the ideal experimental parameters. This statistical technique enables the identification of a combination of factor values that simultaneously optimize several answers while ensuring that each response meets its requirements.

Optimization of study

The optimization process was conducted using mathematical and graphical methods. Fig. 9 illustrates the formulation that yielded the best and most optimal results, as well as the designated design space. Before discovering the optimum formulation, the goal ranges

for responses were determined based on the literature survey. The formulation that has been optimized, is indicated in table 3.

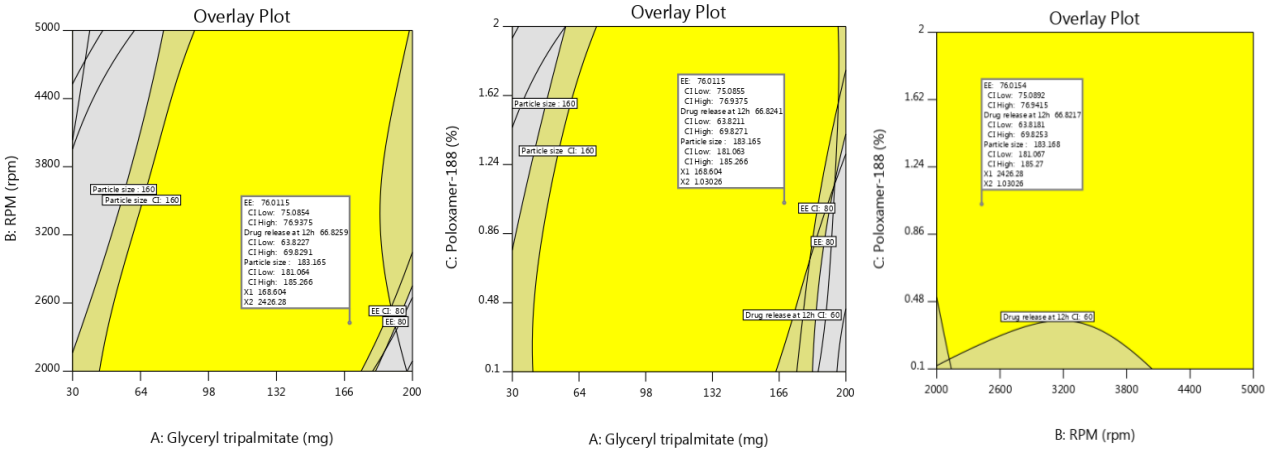

Fig. 9: Overlay plot of region highlighting the optimized space and values

Table 3: Optimization formulation table

Factor	Name	Level	Low level	High level	Std. dev.	Coding
A	Glyceryl tripalmitate	168.60	30.00	200.00	0.0000	Actual
B	RPM	2426.28	2000.00	5000.00	0.0000	Actual
C	Poloxamer-188	1.03	0.1000	2.00	0.0000	Actual

As per the information provided in table 3, the optimized SLN was prepared and responses were recorded in table 4 as observed values. The observed value and predicted mean (obtained from response surface simulation) were compared.

Table 4: Point prediction table of optimized formulation

Response	Predicted mean	Predicted median	Observed	Std dev	SE mean	95% CI low for mean	95% CI high for mean	95% TI low for 99% Pop	95% TI high for 99% Pop
EE	76.0142	76.0142	73.64	0.927832	0.488824	74.8583	77.1701	70.793	81.2354
Drug release at 12h	66.8225	66.8225	68.81	3.00895	1.58525	63.074	70.571	49.8902	83.7548
Particle size	183.168	183.168	203	2.10527	1.10915	180.545	185.79	171.321	195.014

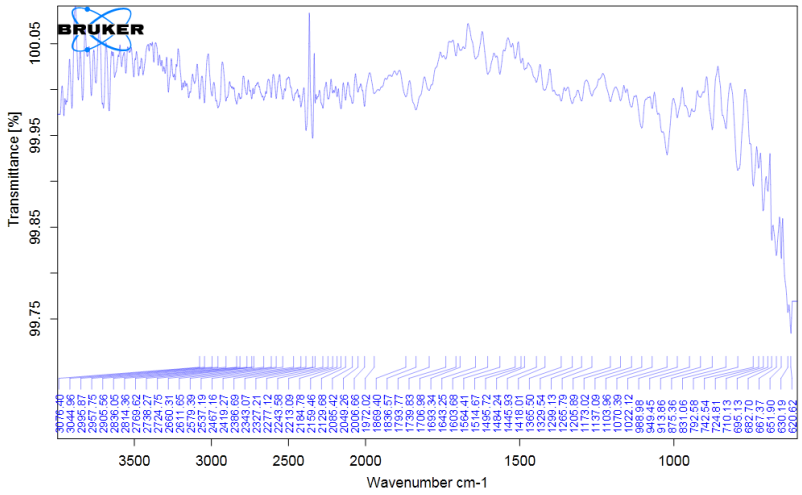

Fig. 10: ATR spectra of gabapentin

ATR study

Sharp infrared spectral peaks in the gabapentin spectrum can be used as a fingerprint to identify GABA in the extrudates (fig. 10). The –NH3+stretching vibration causes an absorption band to appear in the spectra between 3076 and 2814 cm-1. It is possible to attribute the infrared bands at wave numbers of 1564 cm-1 and 1514 cm-1 to-NH deformation vibration. The bands observed corresponded to the asymmetric carboxylate band and/or CH2 deformation band, which formed in the 1500–1350 cm–1 wave number interval. The carbonyl stretch of the COOH group emerged at 1693 cm–1, while the C–N stretch was visible at 1022 cm–1.

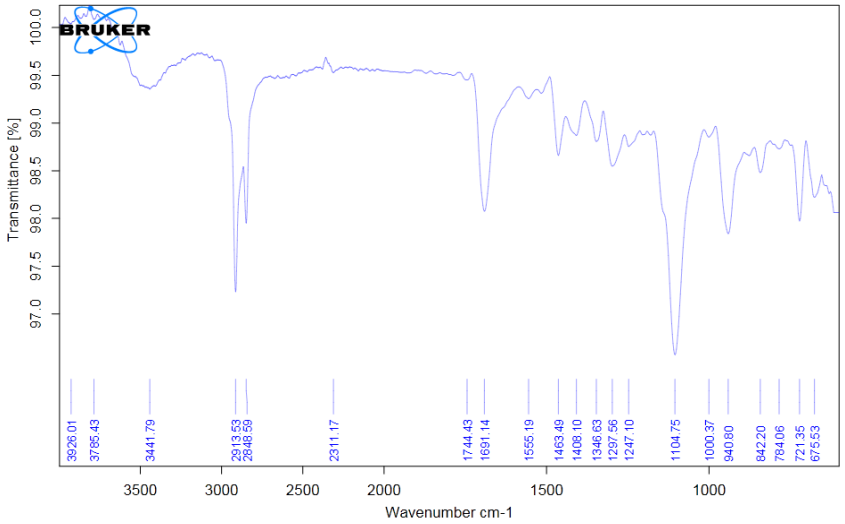

Fig. 11: ATR spectra of optimized formulation

The presence and absence of characteristic peaks were noted from SLN. The –NH3+stretching vibration causes an absorption band to appear in the spectra between 3500 and 3000 cm-1. The IR bands associated with-NH stretching is located at wave numbers of 2913.53 cm-1 vibration. In the 1500 to 1350 cm^{-1} wave numbers interval, the bands observed corresponded to the asymmetric carboxylate band and/or CH^2 deformation band appeared. The C-N stretch at 1104.75 cm^{-1} and the carbonyl stretch of COOH group at 1691.14 cm^{-1} appeared. Similarly, the C–H out-of-plane bending vibrations appeared at 930.80 cm^{-1}. Finally, it found that there are no such major interactions between gabapentin and excipients.

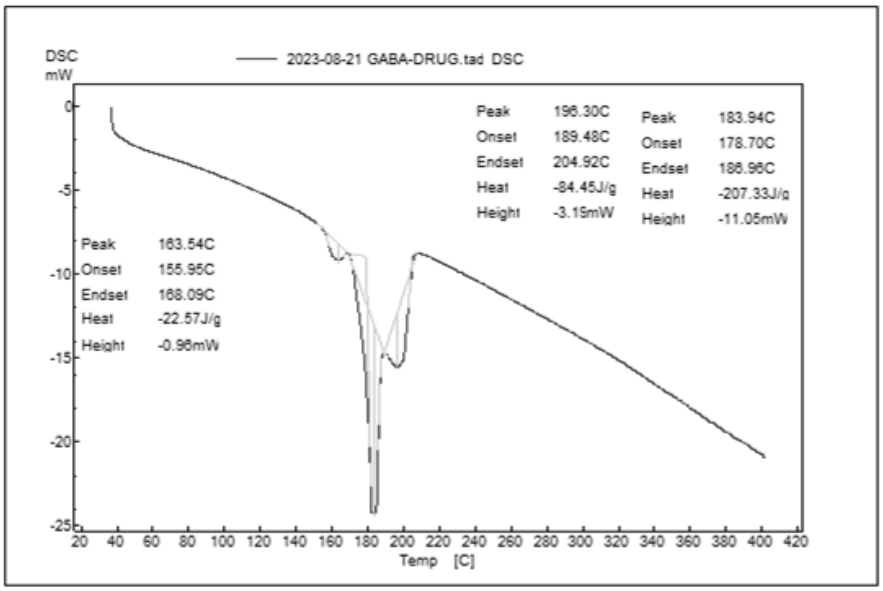

Fig. 12: DSC of gabapentin

DSC study

It observed a sharp endothermal peak at 183.94 °C with heat of energy of-207.33 mJ; which is as per the literature study. It also noted impurity peak at 163.54 °C and a thermal degradation peak appeared at 196.30 °C.

A significant endothermal peak at 208.81 °C, which is close to pure gabapentin as indicated by an earlier measurement of 183.94 °C, was noted in the DSC research (fig. 13). This determined that the endothermal peak had not changed much. It also implied that the pure medication in the SLN formulation would be thermally stable. At 54.26 °C, a large peak was also detected. This peak may have resulted from the complex formed between poloxamer-188 and glyceryl tripalmitate. It was mentioned that sunflower lecithin does not appear to have a pronounced peak.

XRD study

Noted peaks appeared at position 7.731 (2Theta) with high intensity of 21000, 14.84(2Theta) with intensity of 5000, 16.70 (2Theta) with intensity of 1900, 20.14 (2Theta) with intensity of 4000, 23.04 (2Theta) with intensity of 3000, 25.62(2Theta) with intensity of 1800 and at 26.68 (2Theta) with intensity of 2000. A few more characteristic peaks appeared at 29 (2Theta), 30 (2Theta), and 36 (2Theta) with intensity below 500.

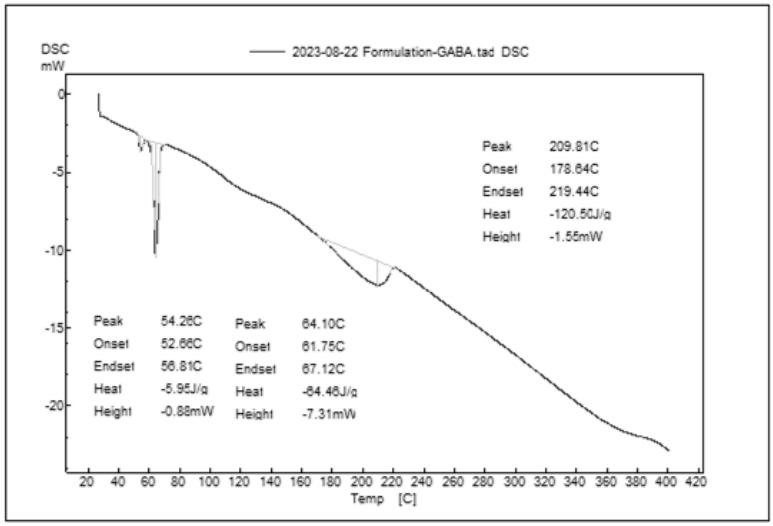

Fig. 13: DSC thermogram of optimized formulation (SLN)

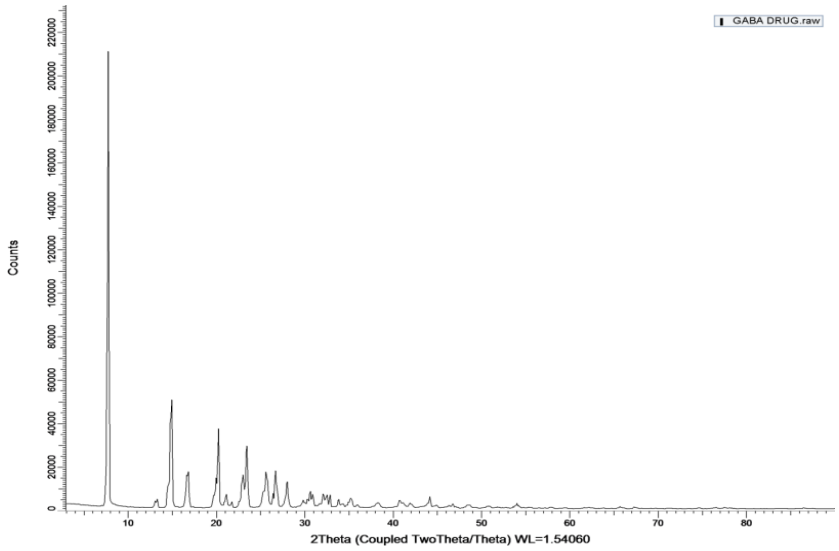

Fig. 14: XRD of gabapentin

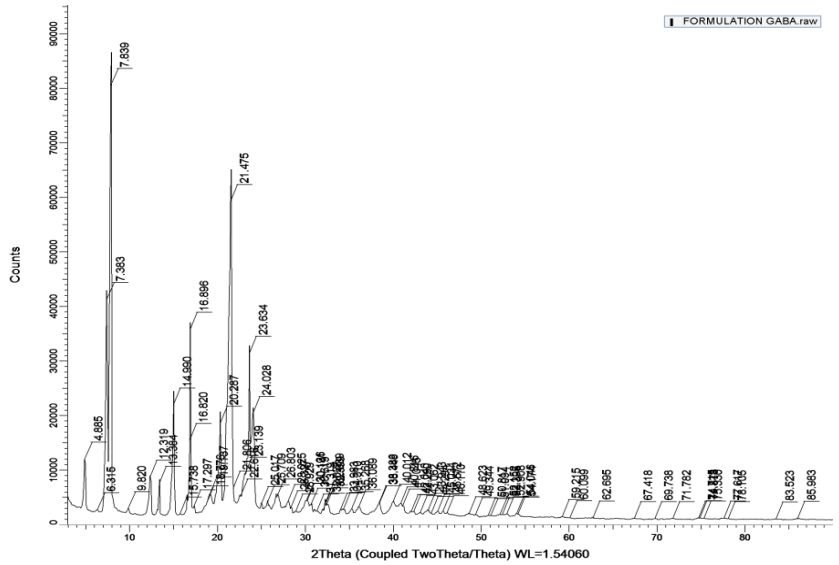

Fig. 15: XRD spectra of optimized formulation (SLN)

The purpose of the XRD study was to trace pure drug in SLN formulation. Significant distinctive peaks were identified in the XRD investigation (fig. 15), and they were identical to pure gabapentin at positions 7.83, 14.99, 16.89, 20.28, and 21.45 (2Theta). This indicated the presence of pure gabapentin in the crystalline arrangement. However, a few more peaks of intensity reduced to below 3000 were observed; which could be due to the presence of solvent and reduced crystallinity during formulation development.

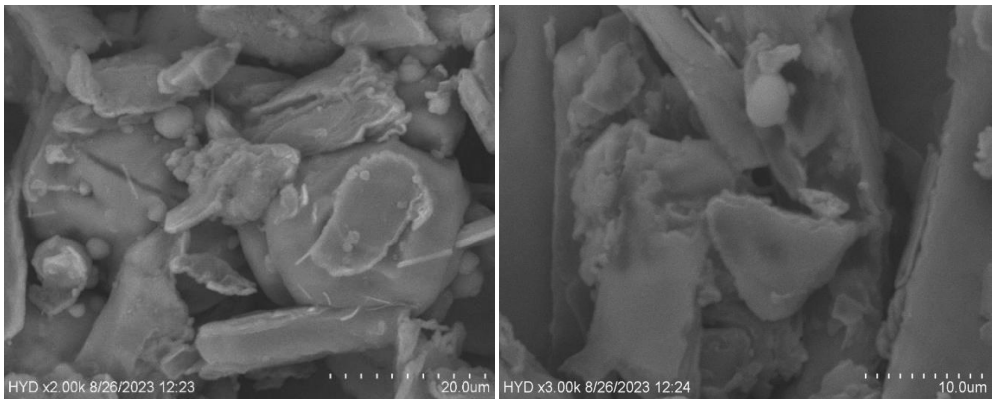

Fig. 16: SEM study of optimized formulation at (a) 20.0 µmand (b)10.0 µm

Surface morphology of optimized formulation

SEM analysis revealed SLN and drug crystals dispersed widely. The analysis also showed that optimized SLN surfaces and appearances are asymmetrical. As seen in fig. 16(a), there is a greater asymmetry in the distribution of SLN across the sample. The optimized SLN formulation was reported to exhibit scattered dispersion in fig. 16(b) (10.0 µm resolution).

Particle size and distribution study of optimized formulation

The optimized formulation's average size was found to be 203.4 nm by the particle size analysis. In a similar way, the Polydispersity Index (PI) came back with a 0.426 result. According to published research, a PI value of less than 0.5 denotes homogeneous dispersion, which is what our formulation showed [29].

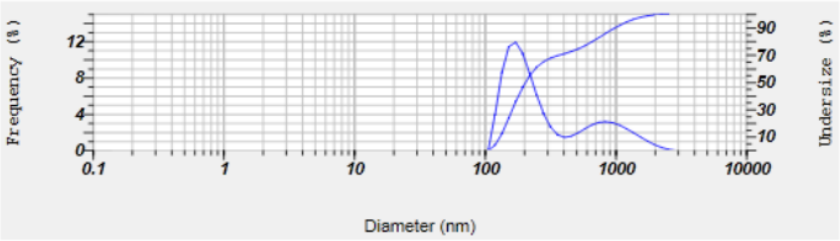

Fig. 17: Particle size and distribution study of optimized formulation

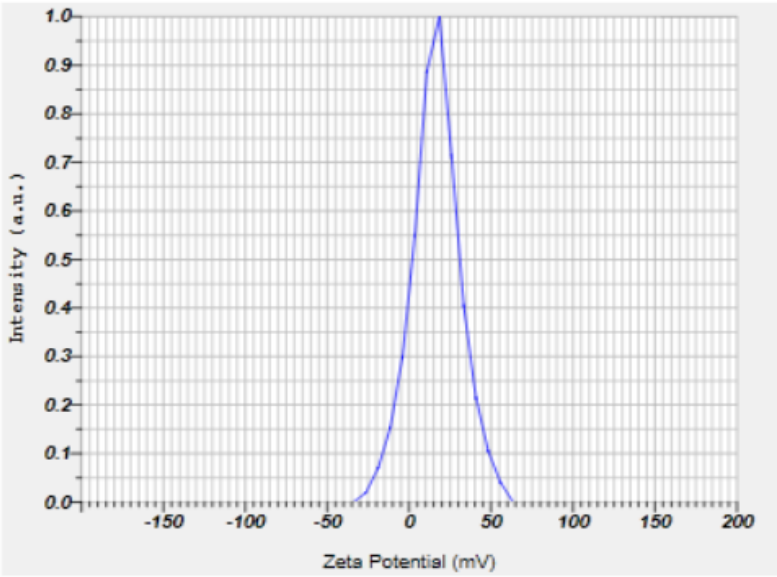

Fig. 18: Zeta potential estimation of optimized formulation

Zeta potential of optimized formulation

SLNs dispersed in phosphate buffer pH 6.8, were used for estimation of zeta potential. Literature review already stated that the values above ±15mV are stable and can be dispersed without raising the stability issue. The study showed a zeta value of 16.5 mV; indicating stability as per the literature available [30].

Table 5: Effect of optimized SLN on picrotoxin-induced convulsive seizure in rats

Group	Treatment	Onset of seizure (min)#	Seizure (%)	Death (%)	Time of death (sec)
Group 2	Disease Control (Picrotoxin)	6.52±0.62	100	100	750
Group 3	Standard drug Treatment (Diazepam)	15.27±0.79$^{\alpha}$	100	16$^{\alpha}$	5200$^{\alpha}$
Group 4	Gabapentin 5.0 mg/kg/day (Optimized SLN formulation)	9.86±0.86$^{\beta}$	100	66$^{\alpha}$	3870$^{\alpha}$
Group 5	Gabapentin 10.0 mg/kg/day (Optimized SLN formulation) High dose	13.63±1.01$^{\alpha}$	100	50$^{\alpha}$	4210$^{\alpha}$
Group 6	Gabapentin 50.0 mg/kg/day (Optimized SLN formulation) Very high dose	14.27±0.75$^{\alpha}$	100	33$^{\alpha}$	4600$^{\alpha}$

Data are presented as mean±SD (n = 6) and were analyzed using an ANOVA followed by Tukey's post hoc test at p<0.05, where $^{\alpha}$P<0.001, $^{\beta}$P<0.01 vs picrotoxin and bicuculline.

Table 6: Effect of optimized SLN on bicuculline-induced convulsive seizure in rats

Group	Treatment	Onset of seizure (min)	Seizure (%)	Death (%)	Time of death (sec)
Group 2	Disease control (Bicuculline)	2.03±0.07	100	100	550
Group 3	Standard drug treatment (Diazepam)	11.76±0.63$^{\alpha}$	100	33$^{\alpha}$	5300$^{\alpha}$
Group 4	Gabapentin 5.0 mg/kg/d (Optimized SLN formulation)	5.52±0.32$^{\beta}$	100	83$^{\alpha}$	3795$^{\alpha}$
Group 5	Gabapentin 10.0 mg/kg/d (Optimized SLN formulation) High dose	6.34±0.92$^{\alpha}$	100	66$^{\alpha}$	4530$^{\alpha}$
Group 6	Gabapentin 50.0 mg/kg/d (Optimized SLN formulation) Very high dose	8.26±0.15$^{\alpha}$	100	50$^{\alpha}$	4920$^{\alpha}$

Data are presented as mean±SD (n = 6) and were analyzed using an ANOVA followed by Tukey's post hoc test at p<0.05, where $^{\alpha}$P<0.001, $^{\beta}$P<0.01 vs picrotoxin and bicuculline.

Development of picrotoxin and bicuculline-induced seizures is slower. As shown in the tables 5, 6, and fig. 19, the onset of seizure was significantly faster P<0.001 in the picrotoxin and bicuculline-treated group in comparison to the standard group, whereas in the of gabapentin-SLN treatment groups, the onset of seizures were delayed significantly in comparison to the disease control group.

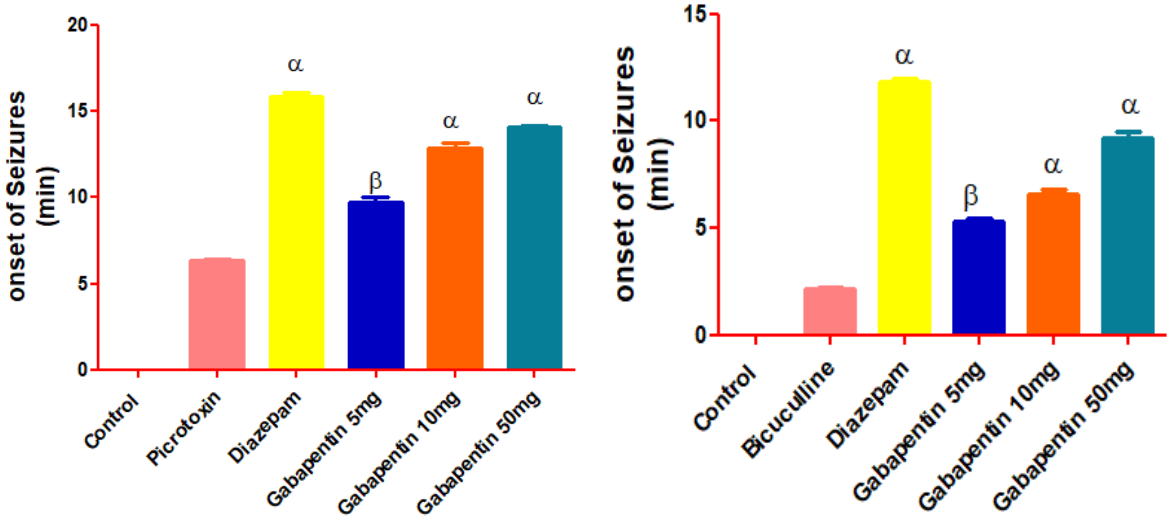

Fig. 19: The effect of gabapentin-SLN on the onset of seizures after the administration of picrotoxin and bicuculline. Data are presented as mean±SD (n = 6) and were analyzed using an ANOVA followed by Tukey's post hoc test at p<0.05, where $^{\alpha}$P<0.001, $^{\beta}$P<0.01 vs picrotoxin and bicuculline

According to the findings depicted in fig. 20, the death percentage in the picrotoxin and bicuculline-treated group is cent percentage where as in the gabapentin-SLN treatment groups death percentage of rats was reduced significantly in comparison to picrotoxin control group.

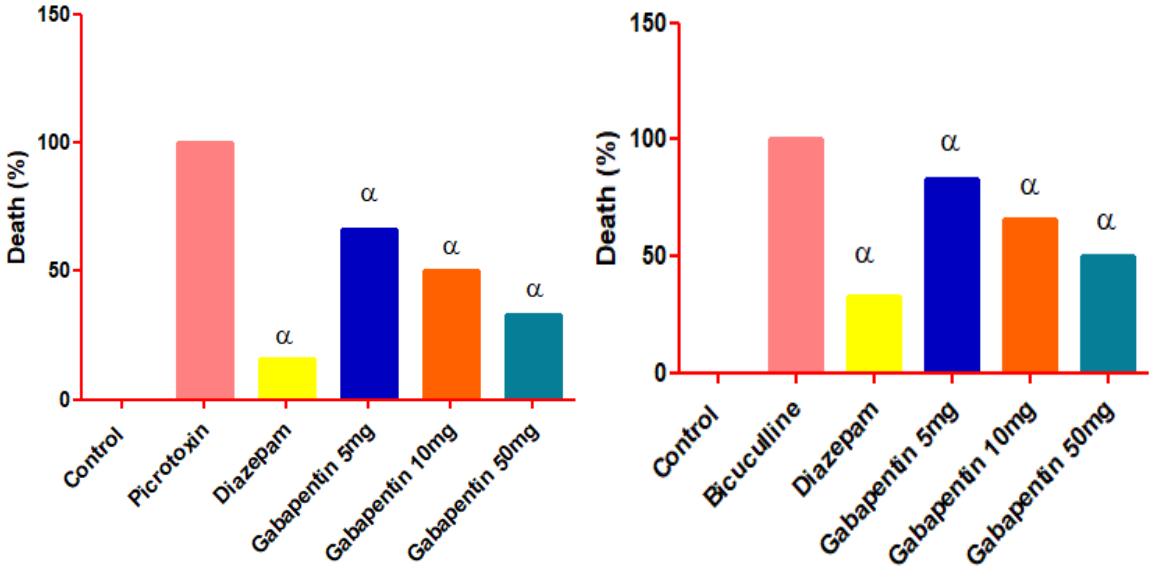

Fig. 20: The effect of gabapentin-SLN on death percentage after the administration of picrotoxin and bicuculline. Data are presented as mean±SD (n = 6) and were analyzed using an ANOVA followed by Tukey's post hoc test at p<0.05, where ᵅP<0.001, ᵝP<0.01 vs picrotoxin and bicuculline

As shown in the fig. 21, the time of death in the picrotoxin-treated group is significantly P<0.001 faster compare to the standard drug group where as in the gabapentin-SLN treatment groups time of death of rats was increased significantly in comparison to picrotoxin control group whereas the time of death in the bicuculline treated group is 30 min-60 min which is faster compare to the standard drug group.

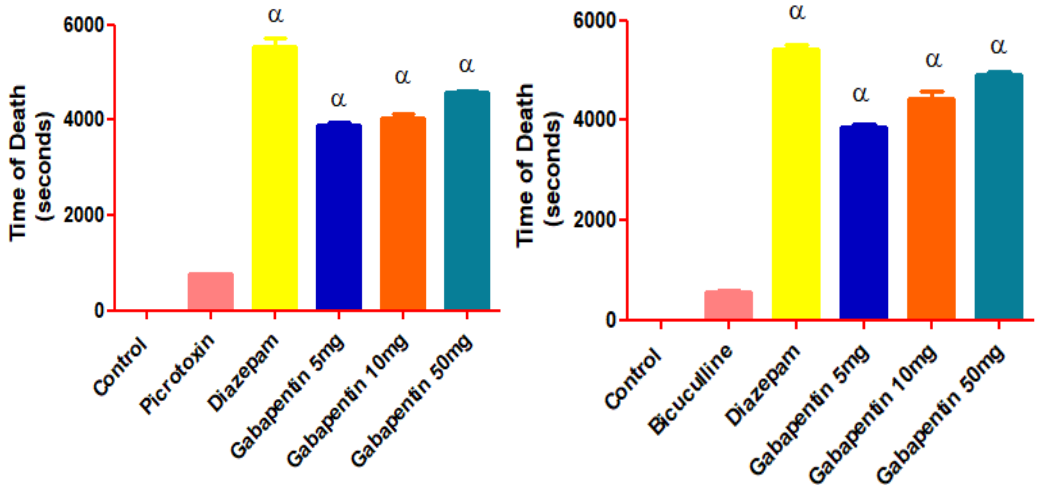

Fig. 21: The effect of gabapentin-SLN on the time of death after the administration of picrotoxin and bicuculline. Data are presented as mean±SD (n = 6) and were analyzed using an ANOVA followed by Tukey's post hoc test at p<0.05, where ᵅP<0.001, ᵝP<0.01 vs picrotoxin and bicuculline

The study conducted by *Kendall et al.* (1981) [31], it was found that the assessment of a compound's anticonvulsant activity encompasses not only its capacity to prevent convulsions but also its ability to postpone the start of seizures, lower mortality rates, and decrease the frequency of these episodes [32]. Hence, the efficacy of our optimized SLN formulation in delaying the initiation of seizures and decreasing mortality rates in the treated animal subjects indicates its potential effectiveness in managing convulsive episodes.

CONCLUSION

The present work successfully loaded gabapentin into rationally designed lipid-based nanovesicles. The microemulsification and ultrasonication were used to formulate 17 different gabapentin-SLN formulations (F1–F17). The entrapment efficiency of the prepared SLNs was high, ranging from 59.58% to 91.26%. The optimized SLN's SEM investigation was found to be asymmetrical. The optimized formulation's average size was found to be 203.4 nm by the particle size analysis, the polydispersity index (PI) of 0.426, and the zeta value of 16.5 mV; indicating stability. When compared to the Bicuculline model, the optimized SLN showed better results regarding the seizure onset in the convulsion caused by picrotoxin.

ACKNOWLEDGMENT

The author acknowledges the School of Pharmacy, Anurag University in Hyderabad, Telangana, India, for all the support.

FUNDING

The authors did not receive any funding for this research work.

AUTHORS CONTRIBUTIONS

The authors report that this publication is based on the first author's Ph. D. thesis (Pooja Agarwal), who conducted the preliminary research, collected the data, carried out the work, and produced the

entire manuscript. The second author (Vasudha Bakshi) was the supervisor, and she revised the text and validated the data for this study. All authors agree with the submission and publication.

CONFLICTS OF INTERESTS

The authors declare that there are no conflicts of interest.

REFERENCES

1. Stafstrom CE, Carmant L. Seizures and epilepsy: an overview for neuroscientists. Cold Spring Harb Perspect Med. 2015;5(6):6:a022426. doi: 10.1101/cshperspect.a022426, PMID 26033084.
2. Praveen P, Panchaksharimath P, Rohith V. Cardiac autonomic dysfunction in patients with epilepsy. Int J Pharm Pharm Sci. 2023;15(10):13-6. doi: 10.22159/ijpps.2023v15i10.49095.
3. World Health Organization. Epilepsy. Fact sheet. Available from: https://www.who.int/news-room/fact-sheets/detail/epilepsy [Last accessed on 07 Feb 2024]
4. Arya RK, Juyal V, Kunwar N. Preparation of carbamazepine chitosan nanoparticles for improving nasal absorption. J Drug Delivery Ther. 2015 May-Jun;5(3):101-8. doi: 10.22270/jddt.v5i3.1090.
5. Lopalco A, Ali H, Denora N, Rytting E. Oxcarbazepine loaded polymeric nanoparticles: development and permeability studies across *in vitro* models of the blood-brain barrier and human placental trophoblast. Int J Nanomedicine. 2015 Mar 11;10:1985-96. doi: 10.2147/IJN.S77498, PMID 25792832.
6. Esfandyari Manesh M, Javanbakht M, Dinarvand R, Atyabi F. Molecularly imprinted nanoparticles prepared by miniemulsion polymerization as selective receptors and new carriers for the sustained release of carbamazepine. J Mater Sci Mater Med. 2012;23(4):963-72. doi: 10.1007/s10856-012-4565-y, PMID 22331374.
7. Leyva Gomez G, Gonzalez Trujano ME, Lopez Ruiz E, Couraud PO, Wekslerg B, Romero I. Nanoparticle formulation improves the anticonvulsant effect of clonazepam on the pentylenetetrazole induced seizures: behavior and electroencephalogram. J Pharm Sci. 2014;103(8):2509-19. doi: 10.1002/jps.24044, PMID 24916334.
8. Jain AS, Date AA, Nagarsenker MS. Design characterization and evaluation of anti-epileptic activity of nanoprecipitating preconcentrate of carbamazepine. Drug Deliv Lett. 2013;3(1):61-9. doi: 10.2174/2210304x11303010009.
9. Ruiz ME, Castro GR. Nanoformulations of antiepileptic drugs: *in vitro* and *in vivo* studies. Methods in pharmacology and toxicology antiepileptic drug discovery; 2016. p. 299-326. doi: 10.1007/978-1-4939-6355-3_16.
10. Sowmya C, Suriya Prakaash KK, Abrar AH. Solid lipid nanoparticles: modern progress in nose-to-brain transduction. Int J App Pharm. 2023 Apr;15(4):20-6. doi: 10.22159/ijap.2023v15i4.47897.
11. Partridge B, Eardley A, Morales BE, Campelo SN, Lorenzo MF, Mehta JN. Advancements in drug delivery methods for the treatment of brain disease. Front Vet Sci. 2022 Sep;9:1039745. doi: 10.3389/fvets.2022.1039745, PMID 36330152.
12. Bhargavi C, Raghuveer P. Enhancing nose-to-brain delivery of piribedil: development of a nanosuspension dispersed in nasal in situ gelling system. Int J App Pharm. 2024 May 7;16(3):86-101. doi: 10.22159/ijap.2024v16i3.50242.
13. Gangurde PK, Kumar L, Kumar L. Lamotrigine lipid nanoparticles for effective treatment of epilepsy: a focus on brain targeting via nasal route. J Pharm Innov. 2019;14(2):91-111. doi: 10.1007/s12247-018-9343-z.
14. Kumar P, Sharma G, Gupta V, Kaur R, Thakur K, Malik R. Oral delivery of methylthioadenosine to the brain employing solid lipid nanoparticles: pharmacokinetic behavioral and histopathological evidences. AAPS PharmSciTech. 2019;20(2):74. doi: 10.1208/s12249-019-1296-0, PMID 30631981.
15. Swidan SA, Ghonaim HM, Samy AM, Ghorab MM. Efficacy and *in vitro* cytotoxicity of nanostructured lipid carriers for paclitaxel delivery. J App Pharm Sci. 2016;6(9):18-26. doi: 10.7324/JAPS.2016.60903.
16. Kelidari HR, Saeedi M, Akbari J, Morteza Semnani K, Gill P, Valizadeh H. Formulation optimization and *in vitro* skin penetration of spironolactone loaded solid lipid nanoparticles. Colloids Surf B Biointerfaces. 2015 Apr 1;128:473-9. doi: 10.1016/j.colsurfb.2015.02.046, PMID 25797482.
17. Ahmed A, Ghourab M, Shedid S, Qushawy M. Optimization of piroxicam niosomes using central composite design. Int J Pharm Pharm Sci. 2013;5(3):229-36.
18. Qushawy M, Nasr A, Abd Alhaseeb M, Swidan S. Design optimization and characterization of a transfersomal gel using miconazole nitrate for the treatment of candida skin infections. Pharmaceutics. 2018;10(1):26. doi: 10.3390/pharmaceutics10010026, PMID 29473897.
19. Knezevic NN, Aijaz T, Candido KD, Kovaleva S, Lissounov A, Knezevic I. The effect of once-daily gabapentin extended-release formulation in patients with postamputation pain. Front Pharmacol. 2019 May 15;10:504. doi: 10.3389/fphar.2019.00504, PMID 31156433.
20. Gad S, Ahmed AM, Ghourab MM, Queshawy MK. Design formulation and evaluation of piroxicam niosomal gel. Int J PharmTech Res. 2014;6(1):185-19.
21. Neves AR, Queiroz JF, Reis S. Brain targeted delivery of resveratrol using solid lipid nanoparticles functionalized with apolipoprotein E. J Nanobiotechnology. 2016;14:27. doi: 10.1186/s12951-016-0177-x, PMID 27061902.
22. Eltahawy NA, Ibrahim AK, Radwan MM, Zaitone SA, Gomaa M, ElSohly MA. Mechanism of action of antiepileptic ceramide from red sea soft coral sarcophyton auritum. Bioorg Med Chem Lett. 2015;25(24):5819-24. doi: 10.1016/j.bmcl.2015.08.039, PMID 26577694.
23. Alhaj MW, Zaitone SA, Moustafa YM. Fluvoxamine alleviates seizure activity and downregulates hippocampal GAP-43 expression in pentylenetetrazole kindled mice: role of 5-HT3 receptors. Behav Pharmacol. 2015;26(4):369-82. doi: 10.1097/FBP.0000000000000127, PMID 25590967.
24. Abd Elghafour BA, El Sayed NM, Ahmed AA, Zaitone SA, Moustafa YM. Aspirin and (or) omega-3 polyunsaturated fatty acids protect against corticohippocampal neurodegeneration and downregulate lipoxin A4 production and formyl peptide receptor-like 1 expression in pentylenetetrazole kindled rats. Can J Physiol Pharmacol. 2017;95(4):340-8. doi: 10.1139/cjpp-2016-0060, PMID 28060522.
25. Aldawsari HM, Eid BG, Neamatallah T, Zaitone SA, Badr JM. Anticonvulsant and neuroprotective activities of *Phragmanthera austroarabica* extract in pentylenetetrazole-kindled mice. Evid Based Complement Alternat Med. 2017;2017:5148219. doi: 10.1155/2017/5148219, PMID 28465705.
26. Gad ES, Zaitone SA, Moustafa YM. Pioglitazone and exenatide enhance cognition and downregulate hippocampal beta-amyloid oligomer and microglia expression in insulin-resistant rats. Can J Physiol Pharmacol. 2016;94(8):819-28. doi: 10.1139/cjpp-2015-0242, PMID 27389824.
27. Shahid M, Subhan F, Ahmad N, Ali G, Akbar S, Fawad K. Topical gabapentin gel alleviates allodynia and hyperalgesia in the chronic sciatic nerve constriction injury neuropathic pain model. Eur J Pain. 2017 Apr;21(4):668-80. doi: 10.1002/ejp.971, PMID 27862616.
28. Joseph E, Reddi S, Rinwa V, Balwani G, Saha R. Design and *in vivo* evaluation of solid lipid nanoparticulate systems of olanzapine for acute phase schizophrenia treatment: investigations on antipsychotic potential and adverse effects. Eur J Pharm Sci. 2017;104:315-25. doi: 10.1016/j.ejps.2017.03.050, PMID 28408348.
29. Scioli Montoto S, Sbaraglini ML, Talevi A, Couyoupetrou M, Di Ianni M, Pesce GO. Carbamazepine loaded solid lipid nanoparticles and nanostructured lipid carriers: physicochemical characterization and *in vitro/in vivo* evaluation. Colloids Surf B Biointerfaces. 2018;167:73-81. doi: 10.1016/j.colsurfb.2018.03.052, PMID 29627680.
30. Garg A, Bhalala K, Tomar DS, Wahajuddin. In situ single-pass intestinal permeability and pharmacokinetic study of developed lumefantrine loaded solid lipid nanoparticles. Int J Pharm. 2017;516(1-2):120-30. doi: 10.1016/j.ijpharm.2016.10.064, PMID 27989820.

31. Kendall DA, Fox DA, Enna SJ. Effect of gamma vinyl GABA on bicuculline-induced seizures. Neuropharmacology. 1981;20(4):351-5. doi: 10.1016/0028-3908(81)90008-3, PMID 7290349.

32. Jahangiri L, Kesmati M, Najafzadeh H. Evaluation of anticonvulsive effect of magnesium oxide nanoparticles in comparison with conventional MgO in diabetic and non-diabetic male mice. Basic Clin Neurosci. 2014;5(2):156-61. PMID 25337374.